heritage

MDPI

Article

Characterization and Analysis of Gypsum Alabaster Constituting the "*Santissimo Salvatore*" Statue by Gabriele Brunelli (Bologna, 1615–1682)

Camilla Favale [1], Gianfranco Ulian [1], Gian Carlo Grillini [2], Daniele Moro [1] and Giovanni Valdrè [1,*]

[1] Department of Biological, Geological and Environmental Sciences, University of Bologna, Piazza Porta San Donato 1, 40126 Bologna, Italy; gianfranco.ulian2@unibo.it (G.U.)
[2] Academy of Fine Art of Bologna, Via delle Belle Arti, 54, 40126 Bologna, Italy
* Correspondence: giovanni.valdre@unibo.it

Abstract

This study is part of a broader conservation and restoration project of the 17th-century statue "*Santissimo Salvatore*" attributed to the Bolognese sculptor Gabriele Brunelli (1615–1682). This sculpture was traditionally classified as a marble statue, i.e., primarily composed of calcium carbonate. However, the careful diagnostic analyses conducted during the present work of restoration revealed that, instead, the sculpture is made of gypsum alabaster, a material predominantly composed of calcium sulphate hydrate ($CaSO_4 \cdot 2H_2O$). In the present research, a multi-analytical investigation was carried out using X-Ray Powder Diffraction (XRPD), Field Emission Environmental Scanning Electron Microscopy (FE-ESEM) with Energy-Dispersive X-ray Spectroscopy (EDS), and confocal Raman microspectrometry. Here, we report detailed and updated analytical data of the material constituting the "*Santissimo Salvatore*" statue by Gabriele Brunelli. These data were found extremely useful to plan and accomplish the restoration work in detail: (i) the suitable conservation project of the artwork, (ii) the reassessment of the knowledge on the artist's sculptural production, and (iii) gaining more information about the material used in the 17th-century Bolognese sculptural context.

Keywords: gypsum alabaster; Gabriele Brunelli; statue; restoration; XRPD; FE-ESEM; raman microspectroscopy; organic contamination

Academic Editor: Marta Manso

Received: 17 November 2025
Revised: 9 December 2025
Accepted: 15 December 2025
Published: 17 December 2025

Citation: Favale, C.; Ulian, G.; Grillini, G.C.; Moro, D.; Valdrè, G. Characterization and Analysis of Gypsum Alabaster Constituting the "*Santissimo Salvatore*" Statue by Gabriele Brunelli (Bologna, 1615–1682). *Heritage* **2025**, *8*, 543. https://doi.org/10.3390/heritage8120543

1. Introduction

The sculpture of "*Santissimo Salvatore*" (Figure 1a) is an artwork made by the sculptor Gabriele Brunelli (Bologna, 1615–1682) that is presently located in the first cloister of the ex-Convent of the Lateran Canons of San Salvatore in Bologna (Via Cesare Battisti 18, Bologna). This location is one of the major monastic complexes, whose history begins in 1149 [1]. However, the original location of the statue was at another site. Indeed, the abbot, Giovanni Crisostomo Trombelli, in 1752 wrote that "*the statue was kept in the first cloister, but was originally in the third cloister*" [2], and this was confirmed by washout signs visible on the surface of the upper part of the sculpture.

The attribution is mainly based on the testimonies of illustrious Bolognese historians of the seventeenth and eighteenth centuries like Carlo Cesare Malvasia, Giovanni Crisostomo Trombelli, and Marcello Oretti. In chronological order, the first document mentioning the statue was written by Carlo Cesare Malvasia in 1686, a few years after Brunelli's death. The document stated "*Le pitture di Bologna che nella pretesa, e rimostrata sin hora da altri*

maggiore antichità, & impareggiabile eccellenza nella pittura, con manifesta evidenza di fatto, rendono il passeggiere disingannato ed instrutto dell'Ascoso Accademico Gelato (Translation: The paintings of Bologna, which, despite the claims and assertions made until now by others of greater antiquity and incomparable excellence in painting, clearly and evidently show the contrary, leaving the passerby disillusioned and enlightened by the Hidden Frozen Academician)" said that "*Nel Chiostro, le tre prospettive a fresco a capo le logge, del Mitelli e Colonna, si come l'ornato a chiaroscuro attorno al nicchio, ove la statua marmorea del Salvatore è del Brunelli* (Translation: In the cloister, the three frescoed perspectives at the head of the loggias, by Mitelli and Colonna, as well as the chiaroscuro ornamentation around the niche where the marble statue of the Savior by Brunelli stands)" [3].

Figure 1. Statue of the *Santissimo Salvatore*. (**a**) Location of the sampling points. (**b**) UV light photograph of the area marked with the rectangle in panel (**a**), showing an orangish colour. (**c**) Example of sample collection with a movable blade scalpel. The labels A–E indicate the positions where the samples were collected.

The *Santissimo Salvatore* was the subject of a restoration approved by the Superintendence for Archaeology, Fine Arts, and Landscape for the Metropolitan City of Bologna and the provinces of Modena, Reggio Emilia, and Ferrara (protocol no. 30182 of 22 November 2022). To design proper conservation and restoration procedures, it is of utmost importance to know the materials used to carve the sculpture. In this context, from the background analysis of historical sources, a debate emerged on the actual material composing the artwork, which was considered marble in most of the documents [2–9]. However, at the beginning of the restoration work, the visual examination of the artwork contrasted this statement [10]. From the macroscopic observations during the initial assessments, an element that raised questions was the surface of the sculpture, which did not show the typical saccharoidal crystalline lustre of marble and, instead, refracted light in a significantly attenuated manner. A further element of perplexity arose from the observation of the distinctive marks on the surface left by the tools used during the creation of the work, which were very deep and marked. This suggested the use of a softer material more prone to being furrowed. Moreover, investigations under ultraviolet light revealed an unusual fluorescence of the stone, with orange hues and yellow inclusions (Figure 1b), diverging from the typical reactions of marble, usually purple, dark violet, or blue.

From these elements, it was necessary to conduct an in-depth diagnostic study, aimed at clarifying the nature of the constituent material and providing a scientific (i.e., mineralogical and materials science) basis for the restoration and conservation of the artwork. For this reason, a multi-methodological mineralogical and materials science diagnostic campaign was devised, employing advanced techniques such as optical microscopy, X-Ray Powder Diffraction (XRPD), Field Emission Environmental Scanning Electron Microscopy (FE-ESEM) with Energy Dispersion X-ray Spectroscopy (EDS) microanalysis, and confocal Raman micro-spectroscopy. By cross-correlating the results from the different instruments, a clearer picture of the materials used by Brunelli to sculpt the "*Santissimo Salvatore*" was obtained, which in turn will guide the restoration intervention in the most accurate and respectful way.

2. Materials and Methods

2.1. Sample Collection from the Statue and Specific Preparation

The samples from the statue of "*Santissimo Salvatore*", shown in Figure 1a, were taken from different areas in order to obtain a representative picture of the type and the conservation state of the materials used to create the manufacture (Figure 1c), to set up the most suitable project of restoration. The sampling was performed in conformity with the UNI EN 16085:2012 "Conservation of Cultural property. Methodology for sampling from materials of cultural property. General rules" [11]. To obtain information on the constituent materials and degradation morphologies, we used, in the present work, advanced diagnostic methodologies like optical microscopy, XRPD, FE-ESEM, EDS, and confocal Raman micro-spectroscopy.

Table 1 and Figure 1a report the details of the location where the samples were collected. Sample A is a white specimen gathered from the vest. Sample B is a grey specimen from the base of the statue. Sample C is another white sample taken from the foot of the *Santissimo Salvatore*, whereas specimen D was collected from the dress and presents dark brown shades on the surface, which are signs of possible alterations. Finally, sample E was carefully taken by removing the layer of deposits from a lateral horizontal area of the dress.

Table 1. Sampling positions and analyses.

Sample	Position of the Sampling	Analyses
A	Yellowish-white sherd from a fracture of the dress	XRPD/FE-ESEM-EDS/Raman
B	Grey sherd from a lacuna of the base	XRPD/Raman
C	White sherd from the right foot	XRPD/FE-ESEM-EDS/Raman
D	Darkened sherd from the internal fold of the dress	XRPD/FE-ESEM-EDS/Raman
E	Black deposits from a horizontal dress fold	XRPD/Raman

All the samples were initially observed in optical microscopy (vide infra) and then ground to a fine powder for XRPD analysis. The ground specimens were prepared with the pestle and mortar technique, obtaining 100 to 200 mg of powder that was then deposited on a glass slide for the diffraction measurements. Furthermore, for both environmental scanning electron microscopy and confocal Raman microspectrometry, a portion of each sample was analyzed as is, using a sterile slide as a sample holder. In addition, samples A, C, and D were analyzed as is for environmental scanning electron microscopy. The specimens were thoroughly analyzed on each side using sterile stainless-steel tweezers for manipulation to avoid any possible contamination.

2.2. Analytical Methods

An Optika ProView B-510 POL series optical microscope with a thread counting lens (4×, 10×, 20×, and 40× magnification) was used for a macro/microscopic documentation of the collected samples. The Optika ProView B-510 POL (Optika S.R.L., Ponteranica (BG), Italy) is a professional-grade trinocular polarizing microscope designed for brightfield and transmitted polarized-light observations, and it was also used for the thin section analysis.

X-Ray Powder Diffraction (XRPD) patterns were collected using a Philips PW 1710 diffractometer (Philips, Amsterdam, The Netherlands) equipped with a graphite monochromator on the diffracted beam. Cu Kα X-rays were generated with a 40 kV and 30 mA power supply. The patterns were collected between 3° and 70° 2θ, with an angular step of 0.02° and an integration time of 2 s. The diffractograms were qualitatively analyzed with the computer program Profex [12], which interfaces with the BGMN program [13] and was used for the identification of the phases in the different samples.

A Field Emission Environmental Scanning Electron Microscope (Quattro S FE-ESEM, ThermoScientific Inc., Waltham, MA, USA), equipped with backscattered electron (BS) and energy dispersive spectroscopy (EDS), was employed to study at high resolution the morphology and local chemistry of the samples. The FE-ESEM analyses were performed in low vacuum conditions, with 70 Pa of water vapour pressure inside the instrument chamber, an acceleration voltage of 12 kV, and a beam current of 1.2 nA. Within these instrumental settings, no conductive coating was needed, obtaining an adequate compromise between imaging resolution and EDS chemical sensitivity.

The Raman microspectrometry was carried out with a WITec alpha300R confocal Raman microscopy system (WITec GmbH, Ulm, Germany), made of an optical microscope and an ultra-high throughput UHTS 300 VIS spectrometer with a CCD camera and gratings of 600 g/mm. A green (532 nm) laser beam source with power output set between 5 mW and 30 mW was used to prevent alterations on the samples (e.g., photobleaching effects). The laser beam was focused on the sample with 20×, 50×, and 100× Zeiss microscope

objectives with a low numerical aperture objective (NA = 0.40) to avoid optical artefacts. The backscattered Raman spectra were collected in confocal mode between 100 and 3900 cm^{-1}, with a resolution of about 2.7 cm^{-1} and an acquisition time of 4 min. The Rayleigh scattering line was removed by an edge filter. Fluorescence effects were minimal in the analyzed samples and did not produce significant masking of the Raman bands. For this reason, apart from the removal of cosmic ray radiation signals, no treatment was applied to the collected spectra.

2.3. Alabaster Geological Provenance

Emilia–Romagna hosts documented occurrences of microcrystalline gypsum associated with the regional gypsum-sulphur formations. Already in the late nineteenth century, Bombicci listed "alabastro gessoso" among the mineral resources of the Bolognese territory and noted its occurrence in small quantities beneath more extensive selenite levels, especially around Tossignano and Imola [14].

The Santerno Valley alignment (Sassatello–Gesso–Pieve di Gesso) represents a distinctive local complex rich in saccharoidal and alabastrine varieties, with historical evidence of use in prestigious architectural contexts such as the municipal staircase in Imola [15].

Additional high-quality alabastrine concretions are reported in the Bolognese *Parco dei Gessi* cave systems (e.g., Spipola and related karst environments) [16].

In eastern Romagna, microcrystalline gypsum associated with the Marecchia area is likewise described as suitable for decorative and monumental applications, and historical sources suggest competing attributions for comparable materials used in major buildings in Bologna (Sassatello versus the Rimini area) [17].

3. Results and Discussion

3.1. Optical Microscopy

Observation of samples A, C, and D collected from the statue revealed a microcrystalline structure significantly finer than that of marble, with no evidence of a saccharoidal texture. Under the stereomicroscope, a microcrystalline structure can be seen with twisted and frayed chalky microcrystals of very fine grain, needle-like in shape, and without any specific and preferential orientation, as well as fine granules of iron oxides and hydroxides and tiny crystals of clay minerals and chalk (Figure 2a). Using a polarizing transmitted optical microscope, a microcrystalline structure can be seen with a felt-like texture represented by chalky microcrystals ranging in size from 0.1 to 0.2 mm, sometimes with a dovetail shape and sometimes highly contorted, and larger grains up to 0.50 mm (porphyroblasts) of selenitic gypsum with a semi-transparent crystalline habit (Figure 2b).

3.2. X-Ray Powder Diffraction

According to the X-ray diffraction analyses carried out on samples A–E, the major mineral constituent is always gypsum, $CaSO_4 \cdot 2H_2O$, as reported in Figure 3a. No diffraction peaks associated with calcium carbonate phases, e.g., calcite, were qualitatively observed in all patterns. In detail, samples A, B, C, and D are entirely made of gypsum, as no peak related to other phases was detected in the diffractograms. As an example, Figure 3b reports the collected diffraction pattern of sample A, which was successively analyzed using a Rietveld refinement protocol. It is possible to note that no other phases than gypsum were identified within the ~1% detection limit of the XRD instrumentation that was employed. However, sample E showed some inhomogeneity, with other diffraction peaks related to weddellite [$Ca(C_2O_4) \cdot 2H_2O$, 20.8 (7)%] and a minimal percentage of quartz [SiO_2, 5.2 (6)%], as detailed in Figure 3c. The presence of the weddellite could be due to the oxidation

of hydrocarbons, the action of lichens, or other organic substances present in polluted environments [18].

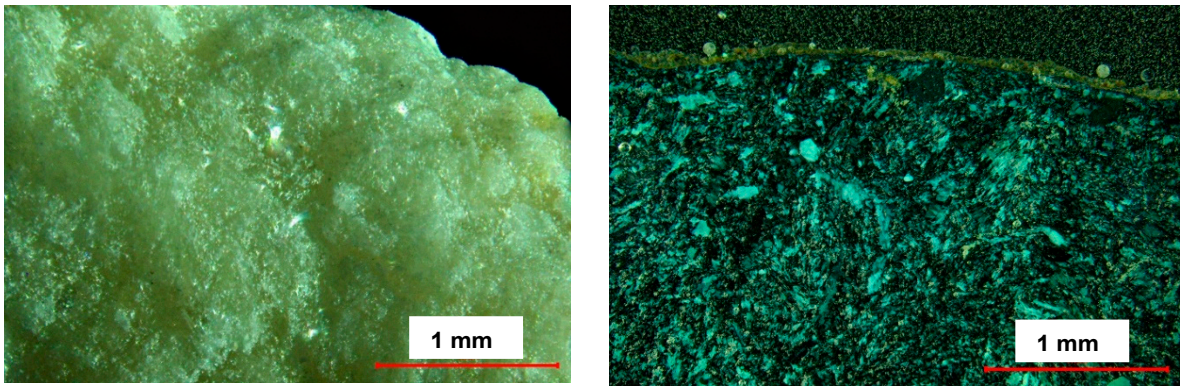

(**a**) (**b**)

Figure 2. (**a**) Stereoscopic optical image of the surface of sample A. (**b**) Polarizing transmitted optical microscopy image of a thin section of sample A.

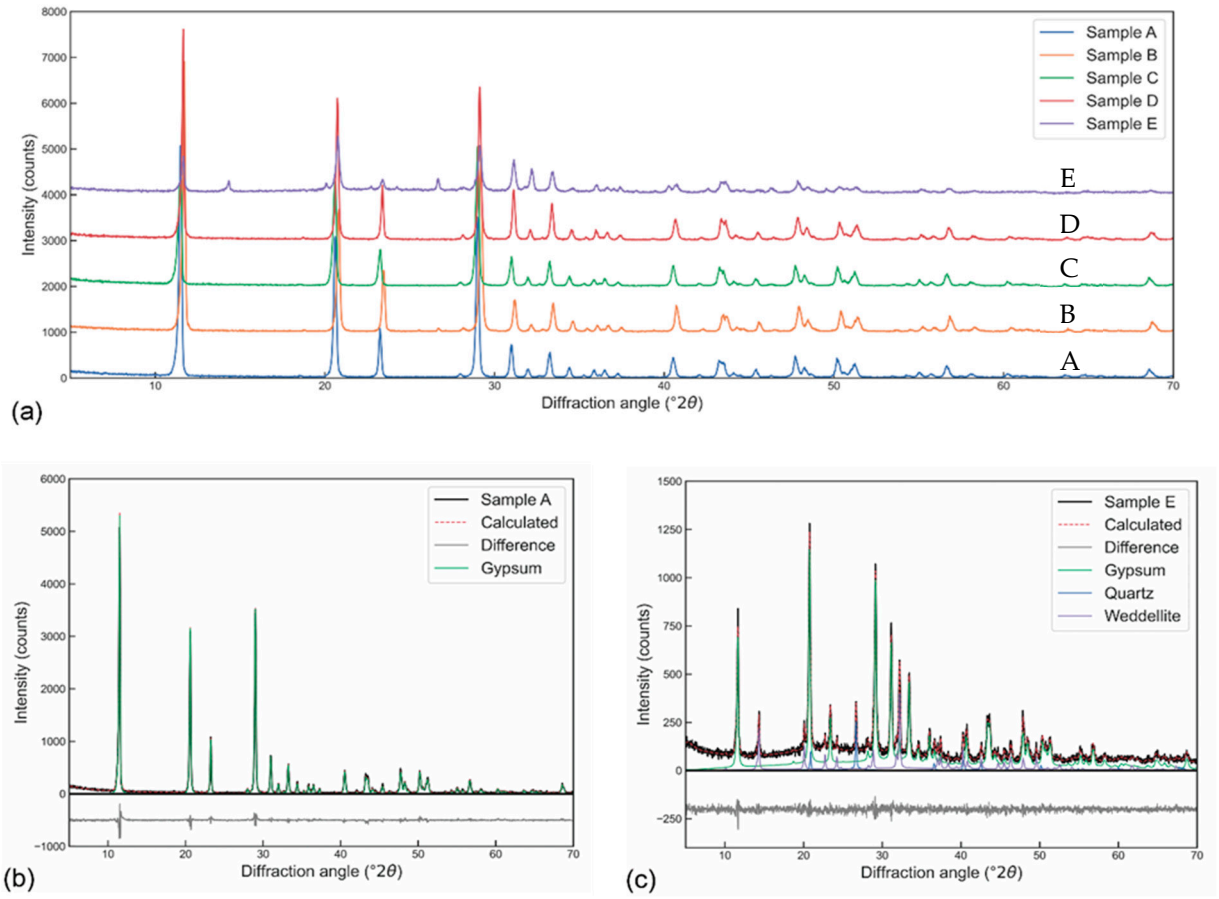

Figure 3. (**a**) Diffraction patterns of the five specimens A–E collected from the *Santissimo Salvatore* statue. (**b**) Rietveld refinement of sample A, showing the presence of only gypsum in the specimen. (**c**) Refinement of the specimen labelled as E, presenting other minor phases.

3.3. FE-ESEM, EDS

An example of FE-ESEM analysis of sample C (sherd from the right foot) is shown in Figure 4, where it is possible to note the presence of large crystals with well-developed

faces and some conchoidal fractures, together with contiguous parallel planes well visible in Figure 4a. Both morphologies are typically found in gypsum, with the former associated with {010}, {011}, {−102}, and {*hk*0} prisms and the second one related to a thin, tabular, almost micaceous, crystal growth. The local mean atomic number revealed by backscattered electron imaging (Figure 4b) shows an almost constant chemistry, with some brighter areas related to the presence of heavier elements. According to the EDS analyses of points 1 (Figure 4c) and 2 (Figure 4d), marked in the BSE image of Figure 4b with black crosses, the dark grey areas contain Ca, S, and O as major elements, whereas the bright spots also contain some amount of strontium (Sr). This analysis, together with the XRD patterns, confirms gypsum as the main constituent of the stony material and suggests the presence of some celestine ($SrSO_4$) that formed together with $CaSO_4 \cdot 2H_2O$ due to possible impurities in the starting materials (gypsum powders or water). The systematic absence in the X-ray diffractograms of reflection peaks related to the phase of celestine confirmed the low amount of that mineral in the sample (powder XRD detection limit of about 1%).

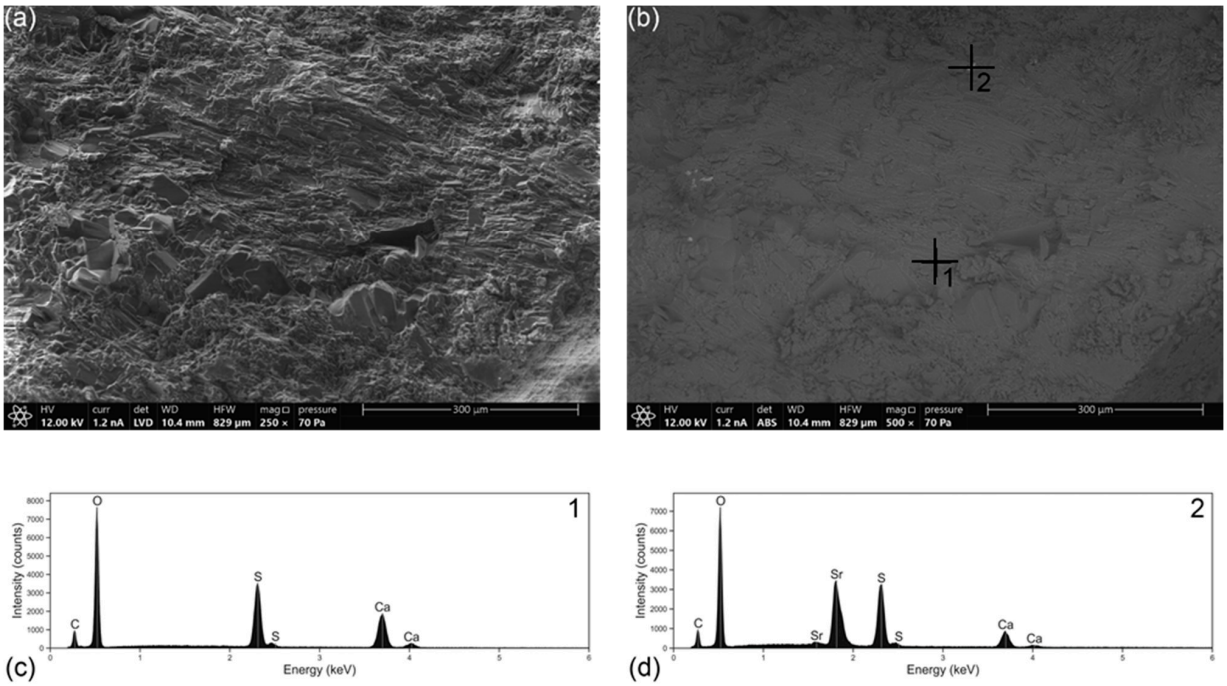

Figure 4. FE-ESEM images of (**a**) secondary electrons and (**b**) backscattered electrons of an area of a small sherd taken from the right foot of the statue (Sample C). Panels (**c**) and (**d**) report the EDS spectra of points 1 and 2, respectively, marked with the crosses in panel (**b**).

The analysis of the darker specimens revealed several differences in the morphology and contents. A representative FE-ESEM-EDS analysis of the dark brown area of sample D (collected in a darkened area in the fold of the dress) is shown in Figure 5, where, using the same scale as Figure 4 (marker of 300 µm), the morphology of the crystals is very different, with a smaller crystallite size and no regular shape. The backscattered electrons image (Figure 5b) highlighted (i) a general matrix of calcium sulphate, i.e., gypsum (point analysis 1, Figure 5e); (ii) a bright area presenting a chemistry compatible with celestine ($SrSO_4$, Figure 5f); (iii) black elongated crusts several microns long with high C and N contents compatible with an organic contamination/degradation (Figure 5g); and (iv) several voids/holes with diameters of about 2–3 µm over all the sample surface. A magnification of the lower part of the crust obtained from secondary electrons and backscattered electrons (Figure 5c,d, respectively) highlights the amorphous nature of the organic material, which is also partially covered with small crystallites of gypsum.

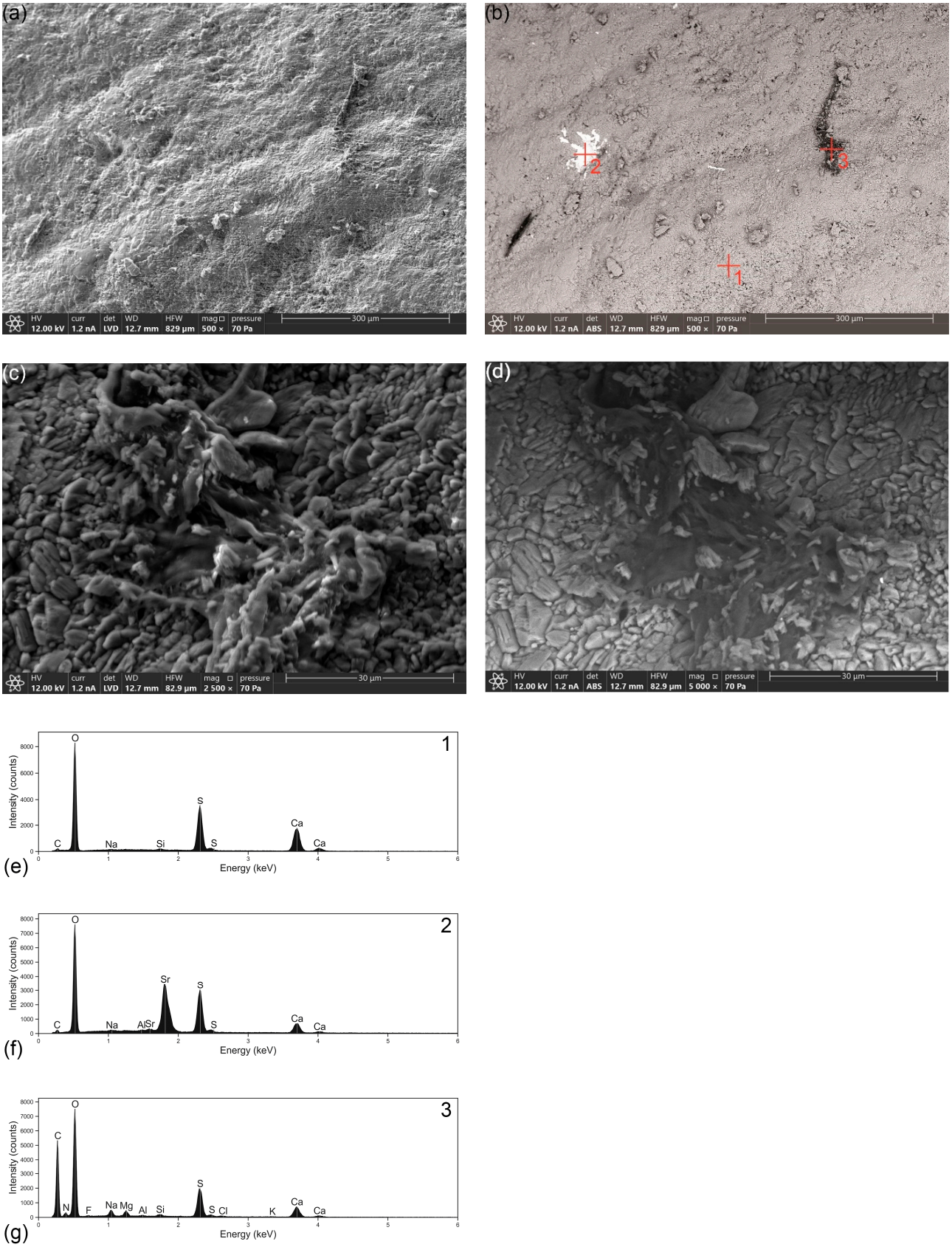

Figure 5. (**a**) Secondary electrons and (**b**) backscattered electrons image of a significant area of sample D, showing the presence of inhomogeneities with dark and bright contrasts. Panels (**c**) and (**d**) show SE and BSE pictures of a zoom of the area of the dark inhomogeneity on the right of panel (**b**). EDS spectra collected at points 1–3 highlighted with crosses in (**b**) are reported in panels (**e**–**g**), respectively.

Sample A, which was collected in a fracture of the dress, showed a morphology that is similar to that of sample D (Figure 6a,b), with gypsum as the main mineral phase. However, it was noted that a generalized presence of filament-like structures was not covered by mineral crystallites and had BSE dark contrast (low atomic number) (Figure 6b, point 1). The relative EDS microanalysis (Figure 6c) resulted in high C and O contents and no nitrogen, a composition that is again compatible with organic matter. According to the Raman analysis (see below), these filament-like structures were attributed to cellulose. The typical gypsum EDS spectrum of the main constituting mineral is collected as an example in point 2 of Figure 6b and reported in Figure 6d.

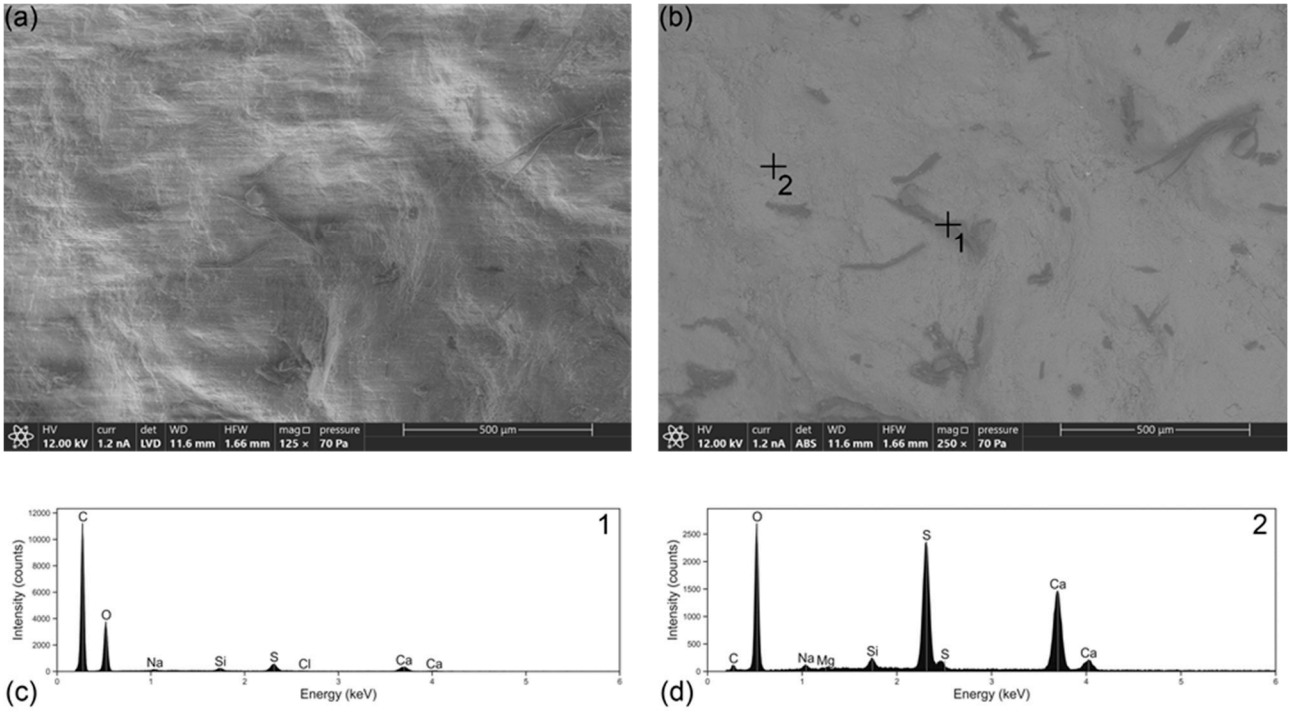

Figure 6. FE-ESEM-EDS analysis of a small sherd taken from the vest of the statue (Sample A). (**a**) Secondary electrons and (**b**) backscattered electrons image of an area where filament-like structures are tens to hundreds of microns long. Panels (**c**,**d**) report the EDS spectra of points 1 and 2, respectively, marked with the crosses in panel (**b**).

3.4. Raman

Figure 7 reports a typical confocal Raman analysis carried out on sample C, where crystallites and assemblages of different sizes are visible (Figure 7a). Figure 7b highlights one of these large crystal assemblages, whose Raman spectrum reported in Figure 7c shows the expected bands of gypsum at 119 cm^{-1} (Ca—SO_4 vibrational mode), 414 cm^{-1} and 493 cm^{-1} [$\nu_2(SO_4)$ symmetric bending modes], 618 cm^{-1} and 670 cm^{-1} [$\nu_4(SO_4)$ asymmetric bending], 1007 cm^{-1} [$\nu_1(SO_4)$ symmetric stretching], and 1135 cm^{-1} [$\nu_3(SO_4)$ asymmetric stretching], according to the results of Raman analyses on gypsum reported in the specific spectroscopy literature [19,20]. The two bands at 3405 cm^{-1} and 3494 cm^{-1} are attributed to $\nu(H_2O)$ stretching modes, with the difference of about 100 cm^{-1} being due to the 0.08 Å difference in the length of O(w)–H···O bonds between non-equivalent OH bonds [21].

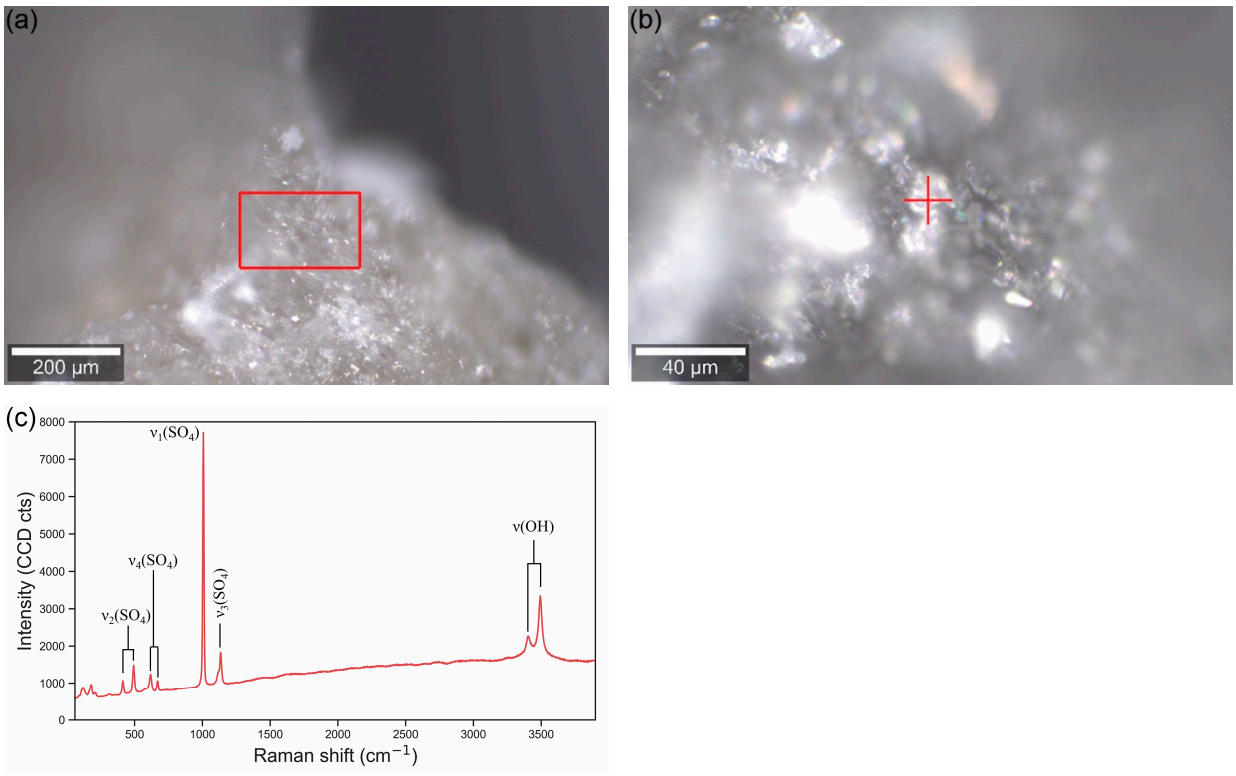

Figure 7. (**a**) Example of an optical picture taken from the sample C. (**b**) Magnification of the area highlighted with the rectangle in panel (**a**). (**c**) Raman spectrum collected on the point marked with the cross in panel (**b**).

Since this organic material was observed in several spots on sample D, often covered by gypsum, and given the non-planar geometry of the specimen, the confocal Raman analysis on this sample was carried out by collecting maps in selected areas that presented almost flat surfaces. An example of these investigations is reported in Figure 8a, where a 20 × 20 µm^2 area was sampled on a 50 × 50 grid of points (pixel resolution of 400 nm). The false colour map (see also a high magnification image of Figure 8a reported in Figure 8b) was obtained from the different spectra (components) found in the points of the area by the green laser spectrum. The colours of the spectra shown in Figure 8c are associated with the colours of the map. From the component analysis, it is possible to note three components (red, blue, and cyan) that present almost identical features, but the intensity of the Raman bands because of the different orientation of the crystallites. The fourth component (with green colour) presents, most notably, in addition to gypsum, the presence of two broad bands between 1200 and 1800 cm^{-1} and three less intense, wide bands at about 2740 cm^{-1}, 2890 cm^{-1} and 3073 cm^{-1}, compatible with an organic contamination. In addition, the width of the most intense band of gypsum (1007 cm^{-1}), modelled from a pseudo-Voigt peak function, is about 10 cm^{-1} in the Raman spectra without organic matter and about 20 cm^{-1} in the contaminated spectrum. This suggests that the mineral around the contamination may have lost some crystallinity due to possible degradation. The macroscopic evidence of this degradation is the presence of an anti-aesthetic orange-brown stain spread unevenly over the surface of the artwork. Almost certainly, they are the results of the alteration of an organic substance applied to the surface and easily absorbed through the pores of the stone. Unfortunately, no documents detailing this process have been found. However, it was historically common practice to apply organic substances to sculptures for various purposes. For instance, in the case of holy subjects, the faithful would often touch the sculptures after dipping their fingers in substances (e.g., candle wax). Organic materials

were also used for their water-repellent properties, serving as protective coatings against atmospheric agents. Additionally, some organic substances were applied to enhance the aesthetic appearance of the sculptures by giving them a polished finish.

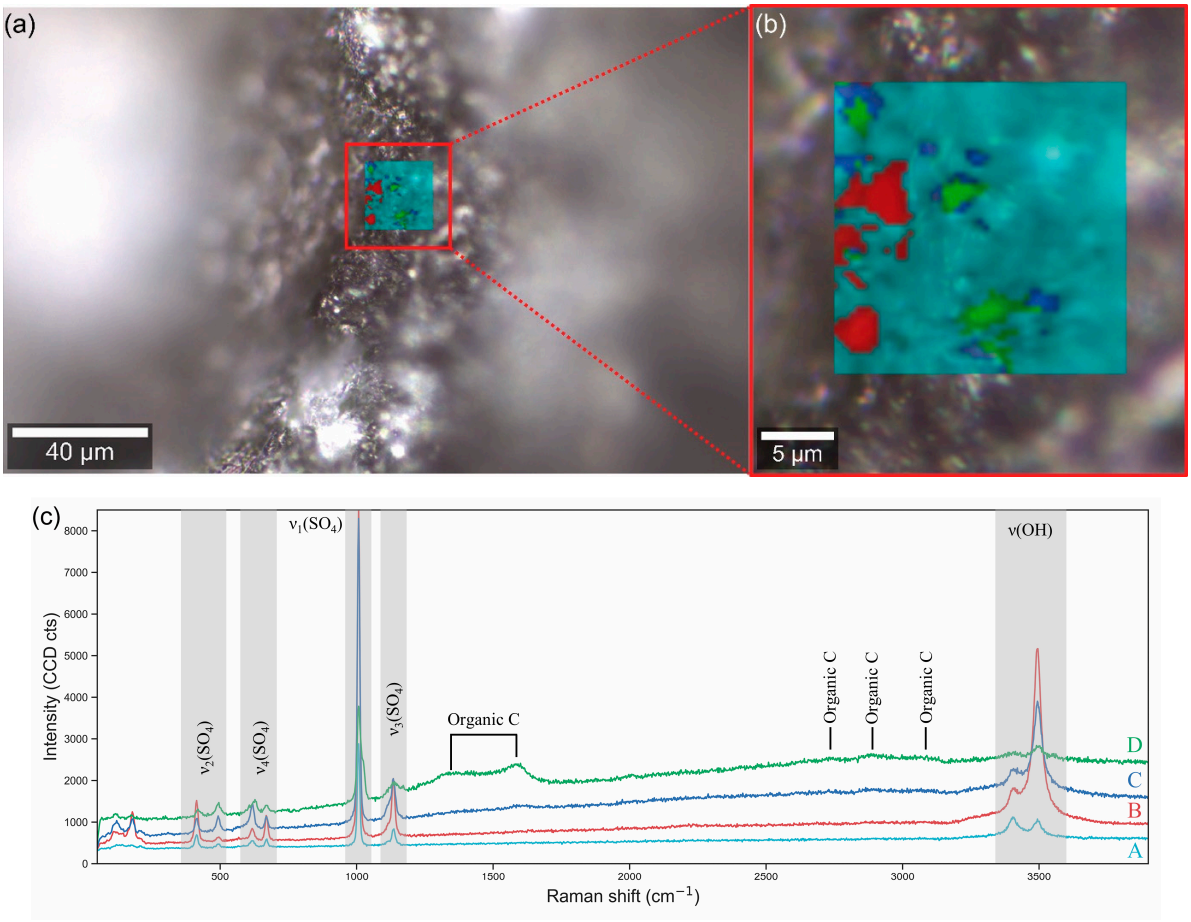

Figure 8. Confocal Raman microscopy map of an area of sample D. (**a**) Overlay of the optical microscopy picture with the combined image obtained from the different components (Raman spectra). (**b**) High magnification of the area highlighted in panel (**a**). (**c**) Raman spectra of the components identified in the false-colour images in (**a**,**b**). The colours of the map in panel (**a**) are the same as those used for the spectra in panel (**b**).

An example can be the "Madonna del Parto" made by Jacopo Sansovino in the Basilica of Sant'Agostino in Rome, which still nowadays has a strong devotional value. Indeed, similar darkened spots were found on the surface, which were the result of the alteration of the candle holy oil that the worshippers used to spread when touching the statue [22].

The same area of sample A analyzed with FE-ESEM was investigated with confocal Raman microspectrometry. For example, Figure 9a,b report a detail of the aforementioned cited filaments. The Raman spectra collected at two different points of the filament are reported in Figure 9c, showing chemical features that are compatible with cellulose, whose specific reference spectrum is reported with a black dashed line in Figure 9c for a direct comparison. Besides the broad band between 3200 and 3600 cm^{-1} attributed to the ν(OH) of water, the main observed bands were at 2895 cm^{-1} [ν(CH) and ν(CH$_2$) stretching]; 1462 cm^{-1} [δ(HCH) and δ(HOC) bending]; 1417 cm^{-1}, 1381 cm^{-1} and 1336 cm^{-1} [δ(HCC), δ(HCO), and δ(HOC) bending]; 1120 cm^{-1} and 1087 cm^{-1} [CC ring breathing]; 971 cm^{-1} [δ(CH) bending mode]; 893 cm^{-1} [δ(HCC) and δ(HCO) bending]; 510 cm^{-1} [δ(COC) bending]; and 456 cm^{-1}, 434 cm^{-1}, and 377 cm^{-1} [ring deformation]. The assignment of the bands to specific normal modes was performed according to previous experimental characterisations [23,24].

A residual band from the $\nu_1(SO_4)$ mode of gypsum was also observed in the spectra. This finding is likely the result of a previous restoration operation, as suggested by the presence of cotton wool residues, which are clearly identifiable due to their stringy structure. Unfortunately, an extensive review of bibliographic and archival sources did not yield any definitive information about past restorations to confirm this hypothesis.

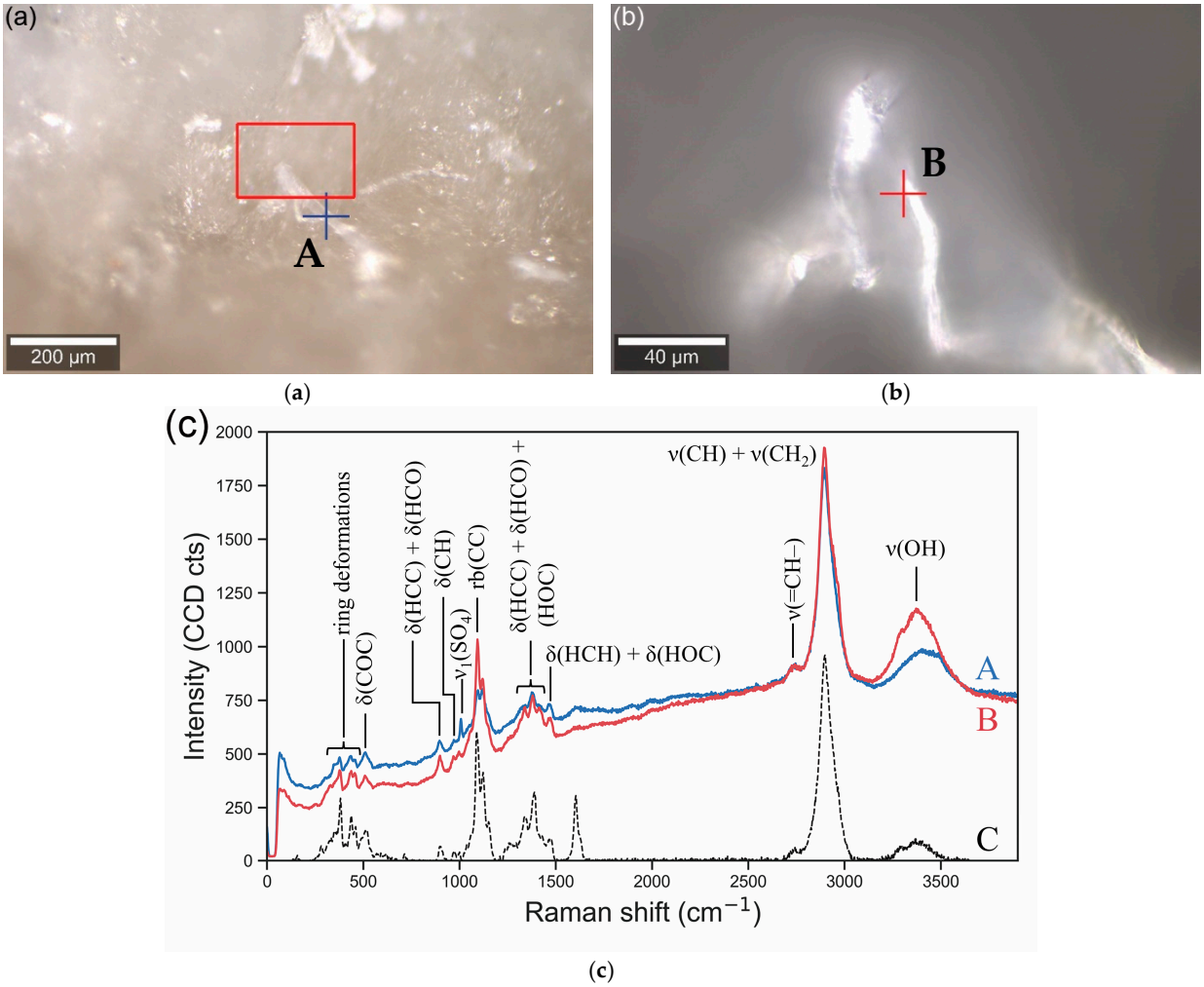

Figure 9. Confocal Raman microspectrometry analysis of the filament-like structures observed in sample A. (**a**) Optical microscopy image of an area of the specimen presenting the filament. (**b**) Zoom of the area highlighted with the rectangle in panel (**a**). (**c**) Raman spectra collected on the points marked with the crosses in panels (**a**) and (**b**) indicated as A and B, together with a reference cellulose spectrum (black dashed line) indicated as C. The colours of the spectra match those of the crosses.

4. Conclusions

The present work reports the results of advanced diagnostic analyses, including FE-ESEM, EDS microanalysis, Raman microspectrometry, and confocal Raman microscopy, used to investigate the material composition and assess the conservation state of the 17th-century statue of the *Santissimo Salvatore*, currently located in the cloister of the former San Salvatore convent in Bologna. The present mineralogical, crystallographic, morphological, and chemical–physical analyses have refuted the historical hypothesis that the artwork was made of marble, indicating gypsum alabaster ($CaSO_4 \cdot 2H_2O$) as the main component. FE-ESEM analyses associated with EDS microanalysis revealed the presence of a material made of large crystals with well-developed faces and some conchoidal fractures, together with contiguous parallel planes, characterized by a minimal percentage of celestine ($SrSO_4$).

Furthermore, the analysis carried out on samples D, collected from the parts of the statue characterized by a dark-brown alteration, showed the presence of an organic contamination of an amorphous nature characterized by high quantities of C, O, and N. In this same area, gypsum crystals appear smaller and irregular in size, sometimes losing their crystallinity as a consequence of degradation. Our multi-methodological study provided important information about the morphology and general characterization of the brown stain, which would be helpful in the future to better understand how they could have been formed. The identification of the sculpture as gypsum alabaster prompted a re-evaluation of the historical attribution of "marble". Indeed, although gypsum was widely used in Emilia–Romagna for stucco and decorative reliefs, its employment in large, free-standing Baroque statuary is much less typical.

These results are of paramount importance both for understanding the artist's material choices and for the development of focused and scientifically based conservation strategies.

Author Contributions: Conceptualization, C.F., G.V. and G.C.G.; methodology, C.F., G.U. and D.M.; validation, C.F., G.U., D.M., G.V. and G.C.G.; formal analysis, C.F., G.U., G.V. and D.M.; investigation, C.F.; resources, G.V.; data curation, C.F., G.U., G.V. and D.M.; writing—original draft preparation, C.F. and G.U.; writing—review and editing, C.F., G.U., D.M., G.V. and G.C.G.; visualization, C.F. and G.U.; supervision, G.V. and G.C.G. All authors have read and agreed to the published version of the manuscript.

Funding: This research received no external funding.

Data Availability Statement: The data reported in this paper are available from the authors on reasonable requests.

Conflicts of Interest: The authors declare no conflict of interest.

References

1. Poli, M. *La Chiesa Canonicale Del SS. Salvatore. Un Complesso Architettonico Innovativo Nel Cuore Di Bologna*; Costa Editore: Bologna, Italy, 2001.
2. Trombelli, G.C. *Memorie Istoriche Concernenti Le Due Canoniche Di S. Maria Di Reno e Di S. Salvatore Insieme Unite*; Corciolani: Bologna, Italy, 1752.
3. Malvasia, C.C. *Le Pitture Di Bologna Che Nella Pretesa, e Rimostrata Sin Hora Da Altri Maggiore Antichità, & Impareggiabile Eccellenza Nella Pittura, Con Manifesta Evidenza Di Fatto, Rendono Il Passeggiere Disingannato Ed Instrutto Dell'Ascoso Accademico Gelato*; Giacomo Monti: Bologna, Italy, 1686.
4. Oretti, M. *Pitture Nelle Chiese Della Città Di Bologna*; Biblioteca Comunale dell'Archiginnasio: Bologna, Italy, 1767; Volume B30.
5. Malvasia, C.C. *Pitture, Scolture Ed Architetture Delle Chiese Luoghi Pubblici, Palazzi, e Case Della Città Di Bologna, e Suoi Sobborghi: Con Un Copioso Indice Degli Autori Delle Medesime, Corredato Di Una Compendiosa Serie de Notizie Storiche Di Ciascheduno*; Longhi: Bologna, Italy, 1782.
6. Oretti, M. *Notizie de Professori Del Disegno Cioè Pittori Scultori Ed Architetti Bolognesi e de Forestieri Di Sua Scuola Raccolte Da Marcello Oretti Bolognese Parte VII*; Biblioteca Comunale dell'Archiginnasio: Bologna, Italy, 1846; Volume B129.
7. Amorini, A.B. *Vite de' Pittori ed Artefici Bolognesi*; Forni: Bologna, Italy, 1843; Volume II, ISBN 978-88-271-1966-2.
8. Riccomini, E. *Ordine e Vaghezza. La Scultura in Emilia nell'età Barocca*; Zanichelli: Bologna, Italy, 1972.
9. Alessandretti, A. Brunelli, Gabriele. In *Dizionario Biografico Degli Italiani*; Istituto dell'Enciclopedia Italiana: Rome, Italy, 1972; Volume 14.
10. Favale, C.; Grillini, G.C.; Valdrè, G. Il Gesso Alabastrino Nella Statua Del Salvator Mundi Di Gabriele Brunelli: Geologia e Mineralogia Di Manufatti Artistici in Emilia-Romagna. In *Torricelliana. Bollettino della Società Torricelliana di Scienze e Lettere di Faenza*; Edit Faenza: Faenza, Itay, 2024–2025; Volume 75–76.
11. *UNI EN 16085:2012*; Conservation of Cultural Property. Methodology for Sampling from Materials of Cultural Property. General Rules. UNI (Unificazione Italiana): Bologna, Italy, 2012.
12. Doebelin, N.; Kleeberg, R. *Profex*: A Graphical User Interface for the Rietveld Refinement Program *BGMN*. *J. Appl. Crystallogr.* **2015**, *48*, 1573–1580. [CrossRef] [PubMed]
13. Bergmann, J.; Kleeberg, R. Rietveld Analysis of Disordered Layer Silicates. *Mater. Sci. Forum* **1998**, *278–281*, 300–305. [CrossRef]

14. Bombicci, L. *Montagne e Vallate Del Territorio Di Bologna: Cenni Sulla Oro-Idrografia, Geologia, Litologia e Mineralogia Dell'Appennino Bolognese e Sue Dipendenze: Con Una Carta Geologica e Una Carta Schematica Di Oro-Idrografia*; Tipografia Fava e Garagnani: Bologna, Italy, 1882.
15. Tomba, A.M. I Gessi Saccaroidi Di Sassatello e Pieve Di Gesso (Vallata Del Santerno). *Rend. Soc. Min. Ital.* **1957**, *XIII*, 374–389.
16. Scicli, A. *L'attività Estrattiva e Le Risorse Minerarie Della Regione Emilia-Romagna*; Poligrafo Artioli: Modena, Italy, 1972.
17. Piastra, S. L'estrazione Del Gesso Nella Romagna Orientale Tra Passato e Presente. In *Gessi e Solfi Della Romagna Orientale*; Memorie dell'Istituto Italiano di Speleologia: Bologna, Italy, 2016; Volume 31, p. 527.
18. AlunnoRossetti, V.; Laurenzi Tabasso, M. Distribuzione Degli Ossalati Di Calcio Mono e 2,25 Idrato Nelle Alterazione Delle Pietre Di Monumenti Esposti All'aperto. In *Problemi di Conservazione*; Compositori: Bologna, Italy, 1973; pp. 375–386.
19. Couty, R.; Velde, B.; Besson, J.M. Raman Spectra of Gypsum under Pressure. *Phys. Chem. Miner.* **1983**, *10*, 89–93. [CrossRef]
20. Saksena, B.D. Raman Spectrum of Gypsum. *Proc. Indian Acad. Sci.—Sect. A* **1941**, *13*, 25–32. [CrossRef]
21. Chio, C.; Sharma, S.; Muenow, D. Micro-Raman Studies of Gypsum in the Temperature Range between 9 K and 373 K. *Am. Mineral.* **2004**, *89*, 390–395. [CrossRef]
22. Ministero della Cultura. *Soprintendenza Speciale di Roma Madonna Del Parto. Un Bio Restauro*; Ministero della Cultura: Rome, Italy, 2023.
23. Wiley, J.H.; Atalla, R.H. Band Assignments in the Raman Spectra of Celluloses. *Carbohydr. Res.* **1987**, *160*, 113–129. [CrossRef]
24. Cabrales, L.; Abidi, N.; Manciu, F. Characterization of Developing Cotton Fibers by Confocal Raman Microscopy. *Fibers* **2014**, *2*, 285–294. [CrossRef]